JOURNAL OF AIRCRAFT
Vol. 46, No. 1, January–February 2009

Engineering Notes

ENGINEERING NOTES are short manuscripts describing new developments or important results of a preliminary nature. These Notes should not exceed 2500 words (where a figure or table counts as 200 words). Following informal review by the Editors, they may be published within a few months of the date of receipt. Style requirements are the same as for regular contributions (see inside back cover).

Analysis of Tethered Aerostat Response Under Atmospheric Turbulence Considering Nonlinear Cable Dynamics

Wanggu Kang* and In Lee†
Korea Advanced Institute of Science and Technology, Daejeon 305-701, Republic of Korea

DOI: 10.2514/1.38599

Nomenclature

A	=	axial aerodynamic force
A_T	=	cross-section area of tether cable
B	=	buoyancy
$\bar{C}$	=	specific length (aerostat hull length)
C_{Dn}	=	cable crossflow drag coefficient
C_{Dt}	=	cable surface drag coefficient
C_{M0}	=	aerodynamic pitching moment coefficient defined at nose
$C_{N,A}$	=	normal, axial aerodynamic coefficient
d	=	cable diameter
E_T	=	elastic modulus of tether cable
N	=	normal aerodynamic force
q	=	aerostat pitching angular velocity
q_0	=	dynamic pressure
S	=	reference area (aerostat hull volume)$^{2/3}$
T	=	tether force
u	=	aerostat axial velocity
$\tilde{u}$	=	tether cable tangential velocity
$\tilde{u}_t$	=	relative cable tangential velocity to airstream
$\tilde{v}$	=	tether cable normal velocity
$\tilde{v}_n$	=	relative cable tangential velocity to airstream
W	=	aerostat weight
w	=	aerostat normal velocity
w_c	=	cable weight per unit length
α	=	angle of attack
ϕ	=	tether cable inclined angle to ground

I. Introduction

THE aerostat is a helium buoyant, aerodynamically shaped and tethered lighter-than-air vehicle. Aerostats are used for advertising, communications relay, surveillance, and scientific observation missions. Aerostats, however, are fairly vulnerable to severe weather. Atmospheric turbulence (in the form of gusts) creates fluctuating load changes in aerostats. The maximum load and fluctuating load magnitude and frequency are major concerns for aerostat structural designers, especially for tether cable designers. A tether cable, which anchors the aerostat to the ground, is a critical part on an aerostat. In the development of an efficient and reliable aerostat, optimized tether cable design is one of the key factors. To ensure that this is possible, it is necessary to estimate the tether reaction force accurately. This can be achieved through a dynamic analysis of the motion of the aerostat under atmospheric turbulence. Different researchers have conducted dynamic behavior analyses of tethered aerostats using various methods (e.g., DeLaurier [1], Jones and Krausman [2], Lambert and Nahon [3], and Stanney and Rahn [4]). Previous research has focused on stability analyses of tethered aerostats. The models developed in these studies focus on aerostat dynamics rather than on tether cable dynamics. As the aerostat operating altitude becomes higher, the tether cable dynamic behavior can be more dominant in the overall tethered aerostat dynamic response. To predict the aerostat response more accurately, the tether cable dynamic model should represent the large movement and extension of the cables. In this work, Bliek's [5] Lagrangian cable dynamic equation is used in a tethered aerostat analysis. A 32 m aerostat developed by the Korea Aerospace Research Institute (KARI) was used in a numerical analysis. The responses of this aerostat under discrete gusts and simulated continuous turbulence were investigated.

II. Dynamic Modeling

A. Nonlinear Tether Dynamic Equations

The cable-body system is considered as a cable problem, as in many previous studies. The dynamic motion of the aerostat provides a boundary condition for one cable end. The tether cable is assumed to move in the vertical plane only. The tether cable is modeled as extensible, highly flexible and segmented, and is expressed in local cable coordinates (Fig. 1). These equations are derived from Bliek [5]. The equation of cable motion moving in a fluid can be expressed in terms of the cable tangential and vertical velocity components $(\tilde{u}, \tilde{v})$, the curvature ϕ, the tension T, and the elongation ε. The gravity and damping forces caused by the relative velocity between the cable and surrounding atmosphere are considered to be external forces in this study,

$$m\left(\frac{\partial \tilde{u}}{\partial t} - \frac{\partial \phi}{\partial t}\tilde{v}\right) = -\frac{1}{2}\rho_{\text{air}} d\pi C_{Dt}\tilde{u}_t|\tilde{u}_t|(1+\varepsilon) + \frac{\partial T}{\partial s} - w_c \sin\phi \tag{1}$$

$$m\left(\frac{\partial \tilde{v}}{\partial t} + \frac{\partial \phi}{\partial t}\tilde{u}\right) = -\frac{1}{2}\rho_{\text{air}} d\pi C_{Dn}\tilde{v}_n|\tilde{v}_n|(1+\varepsilon) + T\frac{\partial \phi}{\partial s} - w_c \cos\phi \tag{2}$$

These force equations should satisfy compatibility equations as follows:

$$\frac{\partial \tilde{u}}{\partial s} - \frac{\partial \phi}{\partial s}\tilde{v} = \frac{\partial \varepsilon}{\partial t} \tag{3}$$

Received 22 May 2008; revision received 4 July 2008; accepted for publication 12 September 2008.

*Ph.D. Candidate, Department of Aerospace Engineering; currently Senior Researcher, Korea Aerospace Research Institute, 115 Gwahangno, Yuseong-gu; wgkang@kari.re.kr (Corresponding Author).

†Professor, Department of Aerospace Engineering, 335 Gwahangno, Yuseong-gu. Associate Fellow AIAA.

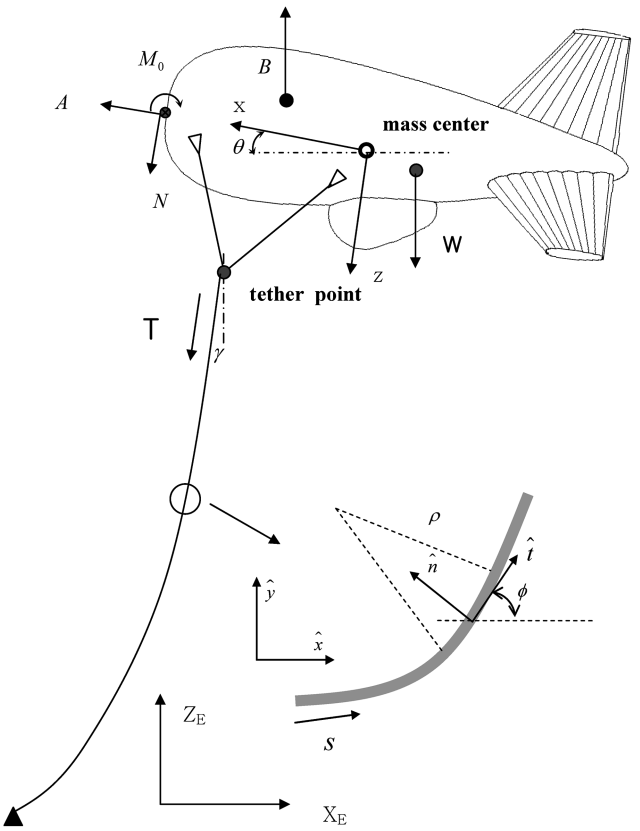

Fig. 1 Schematic diagram of the tethered aerostat model.

$$\frac{\partial \tilde{v}}{\partial s} - \frac{\partial \phi}{\partial s}\tilde{u} = \frac{\partial \phi}{\partial t}(1+\varepsilon) \tag{4}$$

The tension force along the tether cable can be expressed in terms of elongation using the following constitutional equation:

$$T = E_T A_T \varepsilon \tag{5}$$

To simplify the four previous equations, a new vector $\mathbf{Y} = [\tilde{u}, \tilde{v}, \phi, \varepsilon]^T$ is introduced. With the vector $\mathbf{Y}$, the four cable equations can be expressed in a matrix form as follows:

$$M\frac{\partial \mathbf{Y}}{\partial t} + K\frac{\partial \mathbf{Y}}{\partial s} + F = 0 \tag{6}$$

Here,

$$M = \begin{bmatrix} m & 0 & -m\tilde{v} & 0 \\ 0 & m & m\tilde{u} & 0 \\ 0 & 0 & 0 & 1 \\ 0 & 0 & 1+\varepsilon & 0 \end{bmatrix} \tag{7}$$

$$K = \begin{bmatrix} 0 & 0 & 0 & -E_T A_T \\ 0 & 0 & -E_T A_T \varepsilon & 0 \\ -1 & 0 & \tilde{v} & 0 \\ 0 & -1 & \tilde{u} & 0 \end{bmatrix} \tag{8}$$

$$F = \begin{bmatrix} \frac{1}{2}\rho_{\text{air}} d\pi C_{Dt}\tilde{u}_t|\tilde{u}_t|(1+\varepsilon) + w_c \sin\phi \\ \frac{1}{2}\rho_{\text{air}} d\pi C_{Dn}\tilde{v}_n|\tilde{v}_n|(1+\varepsilon) + w_c \cos\phi \\ 0 \\ 0 \end{bmatrix} \tag{9}$$

The implicit finite difference algorithm used to solve Eq. (6) is known as the box method [6]. The tether cable is divided into $N_C - 1$ discrete segments (Δs) before elongation. Each unknown value of vector $\mathbf{Y}$ at time t_{k+1} should be calculated by the known values of $\mathbf{Y}$ at the previous time t_k. To do this, the discrete form of Eq. (6) is used at the midpoint of each time and space step. The discrete form of the midpoint can be approximated by the average value of four surrounding points. Using this approximation scheme, Eq. (6) can be written in a discrete form, as follows:

$$\begin{aligned} &\left\{\frac{1}{\Delta t}(M_{j+1}^{k+1} + M_{j+1}^{k}) + \frac{1}{\Delta s}(K_{j+1}^{k+1} + K_{j}^{k+1})\right\}\mathbf{Y}_{j+1}^{k+1} \\ &+ \left\{\frac{1}{\Delta t}(M_{j}^{k+1} + M_{j}^{k}) + \frac{1}{\Delta s}(-K_{j+1}^{k+1} - K_{j}^{k+1})\right\}\mathbf{Y}_{j}^{k+1} \\ &+ \left\{\frac{1}{\Delta t}(-M_{j+1}^{k+1} - M_{j+1}^{k}) + \frac{1}{\Delta s}(K_{j+1}^{k} + K_{j}^{k})\right\}\mathbf{Y}_{j+1}^{k} \\ &+ \left\{\frac{1}{\Delta t}(-M_{j}^{k+1} - M_{j}^{k}) + \frac{1}{\Delta s}(-K_{j+1}^{k} - K_{j}^{k})\right\}\mathbf{Y}_{j}^{k} \\ &+ F_{j+1}^{k+1} + F_{j}^{k+1} + F_{j+1}^{k} + F_{j}^{k} = 0 \end{aligned} \tag{10}$$

In Eq. (10), there are many nonlinear coupling terms. The mass, spring, and force terms have $(k+1)$ time step unknown values. These nonlinearity terms prevent the use of a direct matrix inverse method to solve Eq. (10). Instead, the Newton–Raphson iteration scheme is used to solve Eq. (10) and calculate the unknown $\mathbf{Y}_{k+1}$ values. The tether cable properties used in this work are summarized in Table 1.

Table 1 Tether cable properties

L	980 m	C_{Dt}	0.035
d	15.8 mm	C_{Dn}	1.17
w_C	300 g/m	E_T	16.3 GPa

B. Aerostat Dynamic Modeling

The aerostat dynamic model used in this paper was obtained by simplifying the three-dimensional 6-degree-of-freedom equation of aerostat dynamics proposed by Lambert and Nahon [3] into a two-dimensional longitudinal aerostat equation of motion. A body fixed frame and an Earth fixed frame are used to describe the aerostat motion as shown in Fig. 1. The body fixed frame is attached to the mass center of the aerostat. In the aerostat, the hull area and hull length are used for the reference surface and the specific length. The aerodynamic forces acting on the aerostat nose are normal, axial forces and the pitching moment is defined at the body fixed frame,

$$N, A = (C_N, C_A) q_0 S \tag{11}$$

$$M_0 = C_{M0} q_0 S \bar{C} \tag{12}$$

The aerodynamic coefficient for the aerostat can be derived by the semi-analytical method proposed by Delaurier [1] or via computational fluid dynamics (CFD) and a wind-tunnel test. Huh et al. [7] conducted a CFD analysis and wind-tunnel test for a 32 m aerostat. The aerodynamic coefficients for the 32 m aerostat from the work of Huh et al. are expressed in the angle of attack as shown later. The dimension of the angle of attack of the 32 m aerostat is in degrees,

$$C_N = -0.0259\alpha + 0.0201 \tag{13}$$

$$C_A = 0.0002\alpha^2 + 0.0004\alpha - 0.0819 \tag{14}$$

$$C_{M0} = -0.0116\alpha + 0.0216 \tag{15}$$

In addition to the aerodynamic force terms, axial and normal force components and resulting moments caused by buoyancy, gravity,

Table 2 32 m aerostat physical dimensions

Buoyancy	1450 kg
Net lift	150 kg
Mass (including added mass)	1640 kg
Inertia (Iyy)	160, 700 kg · m^2
Weight	990 kg
Volume of hull	1746 m^3
Volume of ballonet	624 m^3
Finess ratio	3:1
Hull length	32.8 m
Maximum diameter	10.9 m
Fin area	45.52 m^2

and the tether reaction act on the aerostat vehicle. The longitudinal equations of the aerostat motion can be expressed as follows:

$$-W\sin\theta + B\sin\theta + A + (T\sin\gamma\cos\theta - T\cos\gamma\sin\theta) = m_x(\dot{u} + qw) \tag{16}$$

$$W\cos\theta - B\cos\theta + N + (T\sin\gamma\sin\theta + T\cos\gamma\cos\theta) = m_z(\dot{w} - qu) \tag{17}$$

$$\begin{aligned} &W\cos\theta(r^x_{CG} - r^x_{CM}) + W\sin\theta(r^z_{CG} - r^z_{CM}) \\ &+ (T\sin\gamma\sin\theta + T\cos\gamma\cos\theta)(r^x_{CT} - r^x_{CM}) \\ &- (T\sin\gamma\cos\theta - T\cos\gamma\sin\theta)(r^z_{CT} - r^z_{CM}) \\ &- B\cos\theta(r^x_{CB} - r^x_{CM}) - B\sin\theta(r^z_{CB} - r^z_{CM}) \\ &+ (r^x_{CM}N - r^z_{CM}A) + M_0 = I_{yy}\dot{q} \end{aligned} \tag{18}$$

Here $r^{x,z}_{CG}$, $r^{x,z}_{CM}$, $r^{x,z}_{CB}$, and $r^{x,z}_{CT}$ are the axial and normal lengths from the aerostat hull nose to the center of gravity, mass, buoyancy, and the tether attaching point, respectively. The incoming airspeed of the aerostat is the relative speed between the external wind and the aerostat velocity. The relative airspeed can be obtained by

$$V_{\text{rel}} = [u_{\text{rel}}, w_{\text{rel}}] = V_{\text{as}} - V_{\text{wind}} \tag{19}$$

The angles of attack are related to each relative velocity by

$$\alpha = \tan^{-1}(w_{\text{rel}}/u_{\text{rel}}) \tag{20}$$

The magnitude of the airspeed is

$$U = \sqrt{u^2_{\text{rel}} + w^2_{\text{rel}}} \tag{21}$$

C. Boundary and Initial Conditions

The cable dynamic solution defined by Eq. (10) requires boundary and initial conditions. Boundary conditions for the tether cable are defined at ground and the aerostat attaching point. For the ground, it is possible to use a simply supported condition. The velocities of the cable on the ground connecting nodal point are zero. At the aerostat attaching point, the velocities should match the velocities of the aerostat. The velocity compatibility condition can be expressed as follows:

$$U_{TE} = -(u + q(r^z_{CG} - r^z_{CT}))\cos\theta - (w - q(r^x_{CG} - r^x_{CT}))\sin\theta \tag{22a}$$

$$W_{TE} = (u + q(r^z_{CG} - r^z_{CT}))\sin\theta - (w - q(r^x_{CG} - r^x_{CT}))\cos\theta \tag{22b}$$

The initial conditions should be provided for the tether cable and the aerostat altogether. The initial conditions for the aerostat are calculated for a given external constant wind speed. In a steady state, the derivative terms in the longitudinal equation can be omitted. The trim equation of the aerostat can then be given as

$$\begin{aligned} &W\cos\theta(r^x_{CG} - r^x_{CT}) + W\sin\theta(r^z_{CG} - r^z_{CT}) + B\cos\theta(r^x_{CT} - r^x_{CB}) \\ &+ B\sin\theta(r^z_{CT} - r^z_{CB}) - r^x_{CT}N + r^z_{CG}A + M_0 = 0 \end{aligned} \tag{23}$$

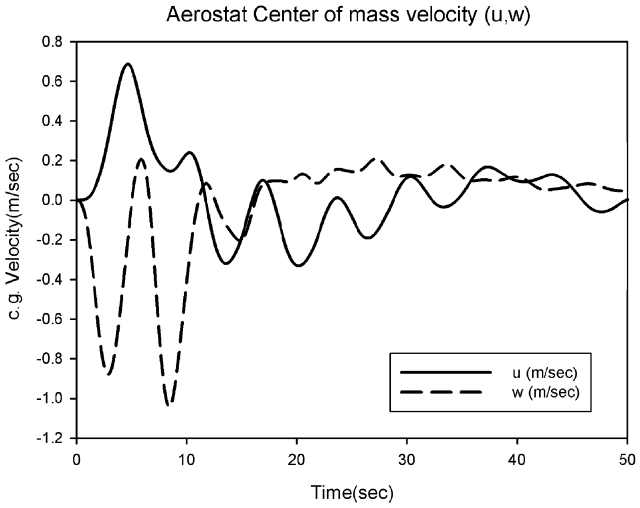

a)

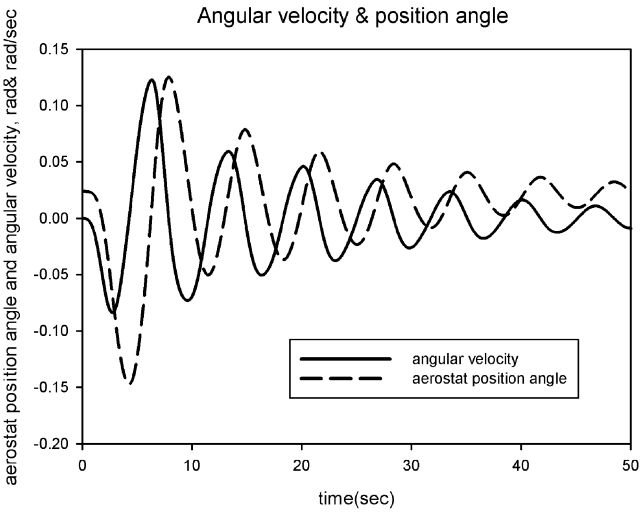

b)

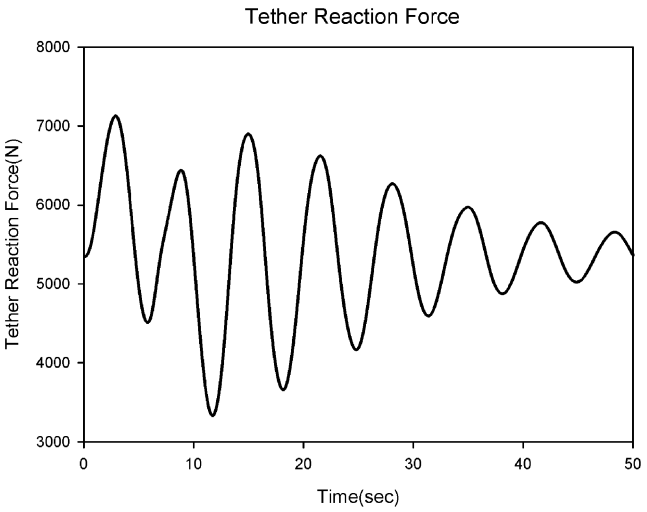

c)

Fig. 2 32 m aerostat motion analysis results. ($U_{\text{wind}} = 20$ m/s, $U_{\text{de}} = 4.11$ m/s, $H = 4$ c).

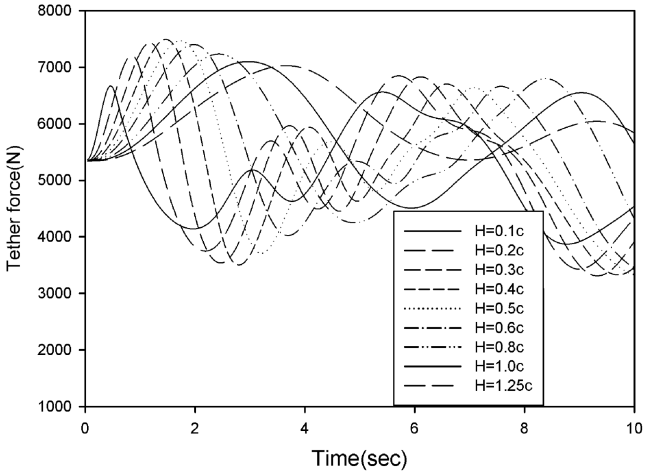

Fig. 3 Tether force time history with various gust scale. (U_{wind}= 20 m/s, U_{de} = 4.11 m/s).

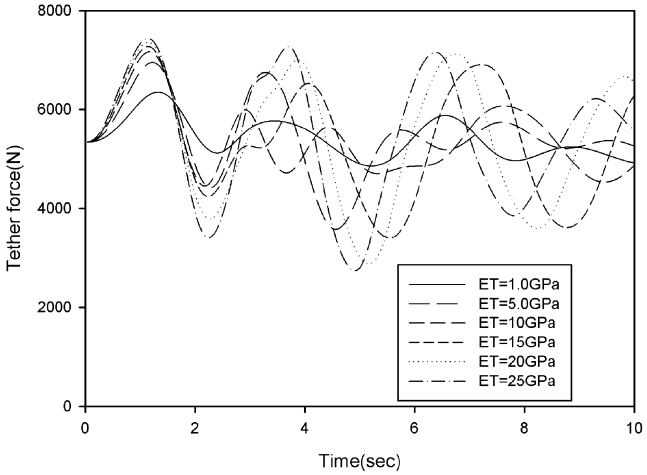

Fig. 4 Tether force time history tether elastic modulus variation. (U_{wind} = 20 m/s, U_{de} = 4.11 m/s).

According to Eq. (23), it is possible to calculate each trim angle for each given external wind condition. With the trim angle, the tether reaction force and the tether cable incline angle can be calculated using Eqs. (16) and (17), respectively, with each derivative term omitted. In this work, the properties of the 32 m aerostat under development by KARI were used. The basic properties of the 32 m aerostat are summarized in Table 2.

III. Numerical Results

MATLAB® was used to build numerical analysis programs for the aerostat and cable dynamics. The aerostat dynamics tests were analyzed using a fourth-order Runge–Kutta method. Only vertical gusts were considered in the aerostat motion analysis. Horizontal gusts and lateral gusts were excluded from the analysis as they have little influence on changes of the tether reaction force. The motions of the 32 m aerostat were investigated under a one-cosine shaped discrete gust, which is defined by the Federal Aviation Administration (FAA) and widely used for small aircraft design. Twenty-four 60-min simulated continuous gust time series using von Kármán power spectral density (PSD) were built to analyze the 32 m aerostat motions under atmospheric turbulence and to monitor the resulting tether reactions.

A. Discrete Gust Analysis

The one-cosine discrete gust profile defined by the FAA is

$$W_{\text{wind}} = \frac{1}{2}U_{\text{de}}\left(1 - \cos\frac{2\pi s}{H}\right) \tag{24}$$

where U_{de} is the maximum vertical gust speed, H is the scale of the gust, and s is the penetrating length into the gust. The FAA defines only the vertical gust speed. For conventional aircraft, the penetrating speed is given by the aircraft speed. For a stationary aerostat, this is not valid. The penetrating speed can be given by the relative speed between the incoming wind speed and the aerostat velocity. The motions of the 32 m aerostat were analyzed under several discrete gust conditions. The defined discrete gust conditions consist of the external wind horizontal speed, the gust scale, and the vertical gust speed. The response of the 32 m aerostat was calculated under a discrete gust with a horizontal wind speed (U_{wind}) of 20 m/s, a gust scale (H) of 131.2 m which is 4 times the aerostat hull length, and a maximum vertical gust speed (U_{de}) of 4.11 m/s. This discrete condition implies that the one-cosine shaped gust passes through the 32 m aerostat in 6.56 s. The velocity of the center of the mass, the angular velocity and position angle, the tether cable reaction force,

Table 3 32 m aerostat dynamic analysis results under simulated turbulence

Gust intensity, m/s	Mean wind speed, m/s	Simulated gust intensity, m/s	Mean value of tether reaction, N	Standard deviation of tether reaction, N
	12.5	0.845	4591.7	436.0
	17.5	0.899	5065.6	477.9
0.9	22.5	0.818	5733.3	407.8
	27.5	0.860	6760.5	341.2
	32.5	0.901	7989.3	363.2
	12.5	1.603	4495.8	757.6
	17.5	1.655	4992.6	832.1
1.7	22.5	1.645	5526.2	804.0
	27.5	1.547	6734.9	667.1
	32.5	1.638	7891.0	662.0
	12.5	2.557	4520.6	1163.2
	17.5	2.356	4993.7	1147.6
2.5	22.5	2.385	5409.3	1143.9
	27.5	2.302	6433.0	1066.6
	32.5	2.327	7783.8	966.5
	12.5	3.227	4885.9	1540.2
	17.5	3.431	4884.5	1462.8
3.3	22.5	3.209	5312.6	1412.3
	27.5	3.480	6782.5	1519.0
	32.5	3.097	7697.1	1329.8
	17.5	3.844	4811.6	1584.7
4.1	22.5	3.816	5475.8	1702.2
	27.5	4.142	6691.1	1851.6
	32.5	4.051	7548.0	1732.4

and the aerostat and tether attaching points were monitored for 50 s, as shown in Fig. 2. Figure 2 shows that the 32 m aerostat passes through the discrete gust starting with a pitch downward movement. Subsequently, all motions are damped out gradually to the initial conditions. The motions of the 32 m aerostat were investigated using a variable gust scale, as shown in Fig. 3. The tether reaction forces of the 32 m aerostat were monitored for 50 s. The maximum tether reaction force increases as the gust scale increases until the gust scale reaches 1.6 times the aerostat hull length. If the gust scale is greater than 1.6 times the aerostat hull length, smaller peak tether reaction forces transpire. The influence of the tether elastic modulus on the aerostat motion was investigated by varying the tether elastic modulus value. The tether reaction forces of the 32 m aerostat were calculated for different tether elastic modulus values from 1 to 25 GPa. As the tether stiffens, the maximum reaction forces increase and the aerostat reacts more rapidly, as shown in Fig. 4.

B. Continuous Gust Analysis

The dynamic motions of the 32 m aerostat were analyzed under a continuous gust. Continuous gust time series for different 10-min mean horizontal wind speed and gust intensities were simulated using the von Kármán vertical gust PSD. The von Kármán gust PSD is represented by L, the gust scale defined at each altitude, and σ_w, the gust intensity defined by the standard deviation of the vertical gust velocity. 1 km gust scale L is defined as 762 m above 1000 ft (304.8 m). The time series satisfying the von Kármán gust PSD can be simulated using Eq. (25) according to Veers [8]

$$x(t) = \sum_{k=1}^{N} \sqrt{2\Omega(\omega_k)\Delta_k\omega}\cos(\omega_k t + \varphi_k) \tag{25}$$

where Ω is the von Kármán PSD function defined for each altitude and gust intensity, ω_k is the kth angular frequency that is equally spaced between the minimum-to-maximum simulating frequency, and φ_k is a random phase angle normally distributed between $-\pi$ to π. The 60-min time series of 24 different turbulence conditions were simulated and used as inputs for the 32 min aerostat dynamic analysis. The resulting tether reactions are summarized in Table 3.

IV. Conclusions

An aerostat dynamic analysis using a nonlinear extensible tether equation has been performed. The response of a 32 m aerostat under a discrete gust and continuous turbulence was computed using the developed analysis computational program. The analysis results show that a nonlinear extensible cable dynamic equation can be used successfully for an aerostat dynamic response calculation. Statistical data of the tether reaction force, the means, and the standard deviation also show that the developed computational program can predict aerostat dynamic behavior under continuous turbulence very well.

References

[1] DeLaurier, J. D., "Prediction of Tethered-Aerostat Response to Atmospheric Turbulence," *Journal of Aircraft*, Vol. 14, No. 4, 1977, pp. 646–651.
doi:10.2514/3.44602

[2] Jones, S. P., and Krausman, J. A., "Nonlinear Dynamic Simulation of a Tethered Aerostat," *Journal of Aircraft*, Vol. 19, No. 8, 1982, pp. 679–686.
doi:10.2514/3.57449

[3] Lambert, C., and Nahon, M., "Stability Analysis of a Tethered Aerostat," *Journal of Aircraft*, Vol. 40, No. 4, 2003, pp. 705–715.
doi:10.2514/2.3149

[4] Stanney, K. A., and Rahn, C. D., "Response of a Tethered Aerostat to Simulated Turbulence," *Communications in Nonlinear Science and Numerical Simulation*, Vol. 11, No. 6, Sept. 2006, pp. 759–776.
doi:10.1016/j.cnsns.2005.01.001

[5] Bliek, A., "Dynamic Analysis of Single Span Cables," Ph.D. Dissertation, Department of Ocean Engineering, Massachusetts Institute of Technology, Cambridge, MA, 1984.

[6] Tjavaras, A. A., Zhu, Q., Liu, Y., Triantafyllou, M. S., and Yue, D. K. P., "The Mechanics of Highly-Extensible Cables," *Journal of Sound and Vibration*, Vol. 213, No. 4, 1998, pp. 709–737.
doi:10.1006/jsvi.1998.1526

[7] Huh, L., Park, Y. M., Chang, B., and Lee, Y., "Aerodynamic Design of the KARI Mid-Sized Aerostat," *KSAS International Journal*, Vol. 7, No. 1, 2006, pp. 43–53.

[8] Veers, P. S., "Modeling Stochastic Wind Loads on Vertical Axis Wind Turbines," Sandia National Lab., SAND83-1909, Albuquerque, NM, Sept. 1984.